Sakarya Journal of Digital Humanities

Publisher: Sakarya University

Vol. 1, No. 1, 12-32, 2026

Research Article

Event-Based Geospatial Assessment of Flood Inundation and Relative Risk in an Urban Watershed: Evidence from Istanbul, Türkiye

Cem Kırlangıçoğlu[1*]
Tauseef Ahmad[2]

[1] Sakarya University, Faculty of Art Design and Architecture, Department of Architecture, Sakarya, Türkiye
kirlangicoglu@sakarya.edu.tr

[2] Central University of Jharkhand, School of Natural Resource Management, Department of Geoinformatics, Jharkhand, India
tauseef.ahmad919191@gmail.com

*Corresponding Author

Received: 18. 04. 2026
Accepted: 11.05.2026
Published Online:19.06.2026

Abstract: Flooding represents one of the most significant global natural hazards, with severe consequences for urban areas. Recent technological advancements and the development of geospatial models have enabled the creation of effective solutions for urban flooding and land use planning in flood-affected cities. The present study employs remote sensing and GIS-based spatial analysis techniques to provide an event-based assessment of flood inundation, exposure, and relative flood risk within the administratively defined urban area of Başakşehir District, Istanbul, Türkiye. Rather than developing a physically based predictive hydrodynamic model, the study aims to identify the spatial distribution of observed flood impacts and their relationship with land use, population exposure, topography, and meteorological conditions. The Multi-temporal Sentinel 1 (SAR) dataset was utilised to extract flood pixels and prepare flood maps, with a pre-flood dataset representing 24.90 km2 of permanent waterbodies, which increased to 45.18 km2 during the flood. The LULC classification of the pre-flood area revealed that the majority of the study area was covered by a built-up area, primarily in the central and southern parts of the territory. During the flood, it was observed that 8.13 km^2 of built-up area and 15.80 km^2 of fallow land were inundated, constituting 60% of the total inundation area. The relative flood risk assessment revealed that Şamlar and the military zone were classified as very high-risk areas, while several central and eastern subdistricts were identified as high-risk areas. The findings of this study are of significant benefit to strategic town planning and disaster management, with the incorporation of further hydrometeorological models serving to enhance the accuracy of the results.

Keywords: Flood Risk, Disaster Management, Land Use Planning, Urban Flooding, Istanbul

1. Introduction

Floods represent the most frequent natural disaster worldwide and a significant hazard in terms of social and economic impacts (Eshrati et al., 2015; Zeleňáková et al., 2017). Floods have a long-term impact on mankind and affect day-to-day life after the event (Hitouri et al., 2024). Therefore, it is imperative to implement comprehensive risk mitigation strategies to address this issue. It has been hypothesised or emphasised that such events are to be expected in locations that are normally arid, where the presence of water is mostly impossible. Such flooding is a consequence of the overflowing of river water during the rainy seasons in numerous countries (Ahmad et al., 2018; Ologunorisa et al., 2022; Shrestha & Kawasaki, 2020). River flooding is the result of a lack of capacity in the streambed to carry large volumes of runoff caused by heavy rainfall or snowmelt (Prokop et al., 2020; Vázquez-Tarrío et al., 2024), and these conditions create natural disasters that are known to result in a significant loss of life and property (Ahmad et al., 2023). This highlights the necessity for the implementation of comprehensive risk mitigation techniques. Among the various types of natural disasters, floods are the most prevalent, representing a hydrological imbalance that results in a multitude of adverse consequences, including mortality, environmental degradation, and disease (Bubeck et al., 2012; Chapi et al., 2017; Mishra et al., 2022).

It is not possible to prevent flooding completely, but it can be predicted and controlled by proper analysis and forecasting methods, and the impact can be controlled (Cloke & Pappenberger, 2009; Tehrany et al., 2015). Recurring floods cause significant damage to transportation, cultural heritage,

Cite as (APA 7): Kırlangıçoğlu, C., & Ahmad, T. (2026). Event-based geospatial assessment of flood inundation and relative risk in an urban watershed: Evidence from Istanbul, Türkiye. *Sakarya Journal of Digital Humanities, 1*(1), 12-32.

This is an open access paper distributed under the terms of the Creative Commons Attribution-NonCommercial 4.0 International License.

environment, economy, and human lives (Abdel-Fattah et al., 2015; Messner & Meyer, 2006; Park et al., 2021). Therefore, a systematic approach is needed to address these challenges and to reduce the residual risk and enhance community resilience. Flood mitigation techniques could be considered by implementing a number of strategies to enhance social capital, capacity building, and psychological resilience. It has been observed that approximately 44% of deaths resulting from natural disasters are attributed to flooding, with the majority occurring in arid regions (Prama et al., 2020). Currently, 800 million people reside in flood-prone areas (United Nations Office for Disaster Risk Reduction, 2015). Every year, 70 million individuals experience the negative consequences of flooding (Kundzewicz et al., 2019). Many nations have significant challenges in managing flood risk, and as the world's population grows and climate change intensifies, so does the urgency in finding a solution (Shalikovskiy & Kurganovich, 2017).

Over the past two decades, there has been a more than twofold rise in the frequency of strong floods, from 1389 to 3254 (Centre for Research on the Epidemiology of Disasters, 2022). This accounts for 44% of all extreme natural occurrences or around 163 floods a year. Floods are more serious than other natural catastrophes, because they claim a higher number of lives (Jonkman, 2005; Hu et al., 2018). Between 2000 and 2019, floods damaged around 1.6 billion people and claimed 104,614 losses of lives (Grigorieva & Livenets, 2022). Floods represent a significant impact in European and Asian countries and create a notable effect on society and the economy due to climate change (IPCC, 2023; Zelenakova, 2011). Asian countries are mostly vulnerable to floods, as major flooding has been reported in Jammu Kashmir and Bihar (India), Egypt, Saudi Arabia, and Indonesia in the last decade, when GIS has emerged as a specific tool to assess and monitor these types of disasters (Abd El Aal et al., 2019; Elsadek et al., 2019; Parida et al., 2022; Rashwan et al., 2023; Sinha et al., 2008). As cities develop and sprawl near river banks, coastal regions and low-lying areas, the populations in those cities are mostly vulnerable to flood (Bigi et al., 2021; Hall et al., 2003). The high population and improper urban sprawl and water management system cause floods in the cities (Dobrovolsky et al., 2018). Precipitation patterns, sea-level rise, and extreme weather events associated with climate change are key factors influencing flood occurrence. These include the intensity, duration, volume, timing, and precipitation type.

Furthermore, temperature patterns can also influence the occurrence of floods. For instance, they can result in the formation of ground freezing, and the melting of snow and ice (Bates et al., 2008). There has been a discernible increase in the frequency and intensity of some severe weather events, such as flash floods and subsequent inundation, as a consequence of global warming (Kundzewicz et al., 2014; Zhao et al., 2023). The exacerbation of flooding by human influence is mainly a consequence of poor land management, deforestation, and urbanisation. These activities alter natural drainage patterns. The phenomenon of rapid economic growth has not only increased the vulnerability of floodplain areas but has also affected the investment in flood risk management infrastructure. The impact of floods has increased in correlation with environmental changes (Ku, 2024; Tomar et al., 2021). Lake Poyang in Southern China has experienced increased flooding in recent decades because of the construction of embankments to protect the rural population that has the effect of reducing the space available to store floodwater, thereby raising the lake level during the summer flood season and increasing the risk of catastrophic dike collapse (Shankman et al., 2006). Nevertheless, it is evident that the observed increase in flood frequency is attributable to a number of factors, including urbanisation and population growth in flood-prone areas, rising property values, and a decline in public awareness of natural hazards. There is a concentration of people and resources in areas with a high risk of flooding in many developing countries, such as Vietnam, Bangladesh, and Cambodia (Peduzzi et al., 2009). These high concentrations of population are due to the human tendency to settle beside river banks, which has been observed in many cities throughout the world, and these cities are more vulnerable to floods (Merz et al., 2021).

In Türkiye, floods represent the second most destructive natural disaster after earthquakes (Koç & Thieken, 2018), whereas the Emergency Events Database (EM-DAT) report in 2023 revealed that the total average annual flood events, including glacial lake outbursts, was 170 between 2003 and 2022. In 2023 alone, there were 164 flood events. Despite the implementation of various preventive measures such as detention dams, river reclamation, and drainage projects, the majority of Turkish cities are becoming more vulnerable to flooding (Balaban, 2016). The increasing irregularity in precipitation increases the frequency of flood events. A significant number of urban areas are at risk of flooding,

and the financial loss caused by flood-related disasters has been monitored (Aslan, 2022). From 1948 to the present, floods in Türkiye have resulted in material losses of approximately 2.5 billion USD and the loss of 1401 lives (CRED, 2022).

In another report by the Turkish Disaster Database, 1076 flood events occurred during the period of 1960–2014, causing a major economic impact of 800 million USD with 795 losses of lives (Koç & Thieken, 2018). Türkiye represents specific climatic, topographic, and geologic variations. The precipitation regimes of several Turkish basins present considerable variations, which result in significant fluctuations in river flow rates. Türkiye's yearly average economic damage from floods is expected to be around 296 million USD as of 2015 (Balaban, 2016). Furthermore, the diminished capacity of riverbeds to receive high runoff volumes results in flooding in mountainous regions (Ahmad et al., 2019). This has become a significant concern for researchers and scientists in these geographical regions. In addition, the unmanaged use of watersheds and the phenomenon of rapid urbanisation have contributed to the occurrence of urban flooding (Yanmaz & Usul, 1999). Furthermore, the concentration of major urban areas in flood plains increases the vulnerability of these locations to flooding. Urban flooding has emerged as a significant concern, particularly in areas with impervious surfaces due to inadequate drainage infrastructure and high rainfall intensity (Guo et al., 2021; Murray & Ebi, 2012).

This results in an elevated runoff in the area, thereby increasing the risk of flooding in urban areas. The impact of rapid urbanisation on urban hydrology and floodplain hydraulics is a significant factor in the management and development of sustainable infrastructure, with the objective of reducing flood vulnerability. Researchers are employing remote sensing (RS) and geographic information systems (GIS) to analyse various terrain-based hydrologic models due to their rapid and precise response. GIS enables users to perform crucial tasks in the context of natural hazards that have a spatial element (Coppock, 1995; Gaya et al., 2023; Korjenić et al., 2021). The technique of flood risk modelling based on digital elevation models (DEM) in GIS has become the principal tool for analysing urban flooding in major cities worldwide, employing Synthetic Aperture Radar (SAR) datasets. GIS has also been employed to characterise watersheds and to conduct related research in hydraulic science. It has the potential to overcome any inequity that may be encountered, enabling researchers to use large datasets and present the pre- and post-flood situation to the user for better understanding and policy-making (Coroza et al., 1997). Therefore, this paper presents an event-based geospatial assessment of flood inundation, exposure, relative flood risk, and meteorological variability for the Başakşehir District of Istanbul, Türkiye.

The implications of SAR Sentinel 1 data have been utilised to delineate the flood-inundated areas, and an impact analysis on the land use and land cover (LULC) has been conducted for the region's potential flooding. The spatial distribution of observed inundation and relative flood risk was quantified through GIS-based overlay and district-level indicator calculations, while meteorological analysis was conducted to interpret the rainfall conditions associated with the flood event. It would be beneficial for urban planners and local authorities to understand the risk areas and implement DEM datasets in the region to effectively address the issue of flood inundation in the future. Considering the data and implementation requirements of hydrological and hydraulic models such as HEC-RAS, HEC-HMS, and SWMM, several studies have employed GIS-based techniques to assess flood impacts in different urban contexts (Ahmad et al., 2019; Tripathi et al., 2019). This study provides a comprehensive assessment of rainfall distribution and its contribution to the flooding in the study area. This study has been initiated for the region and could act as first-hand information for the people and government for mitigation works and be helpful in future studies.

Floods are hydrological phenomena that naturally develop within watershed boundaries rather than administrative boundaries. However, in densely urbanized metropolitan areas, flood impacts, exposure, emergency response, and land-use planning decisions are commonly managed through administrative units. Therefore, the Başakşehir municipal boundary was used as the primary unit of analysis in this study to evaluate the spatial distribution of observed inundation, exposed built-up areas, and relative flood risk from an urban planning and disaster management perspective. To partially account for the broader hydrological context, the analysis also incorporated the Sazlıdere Dam and its surroundings through a 1 km buffer area. Accordingly, the results should be interpreted as an administrative-scale assessment of event-based urban flood exposure, rather than a complete watershed-scale hydrological model. It should be noted that the proposed approach is not intended

to replace physically based hydrological or hydraulic models such as HEC-RAS, HEC-HMS, or SWMM. Instead, the study provides an event-based geospatial assessment derived from observed SAR-based inundation, LULC information, DEM interpretation, population distribution, and meteorological records. Therefore, the results should be interpreted as relative spatial patterns of flood exposure and risk rather than deterministic predictions of flood depth, velocity, or future inundation extent.

2. Material and Methodology

2.1. Study area

Başakşehir is a district located in the European part of Istanbul Province, Türkiye (Figure 1). This study encompasses the Başakşehir District and its surrounding areas in Istanbul Province, situated between 41°2'55'' and 41°12'44''N latitude and 28°37'40'' and 28°51'86''E longitude. The total area of Başakşehir District within the municipal boundary is 104.49 km^2 with a population of 514,900, which was considered for the administrative-scale flood exposure and relative risk assessment (Turkish State Meteorological Service, 2023). Although flood generation and runoff processes are controlled by watershed-scale hydrological and topographical conditions, the present study focuses on the spatial impacts of the September 2023 flood event within the urban administrative unit where land-use planning, emergency response, and disaster risk reduction measures are implemented. Since the observed flood event directly affected Başakşehir District, the municipal boundary was selected as the primary spatial unit of analysis. In order to provide additional hydrological context beyond the administrative boundary, Sazlıdere Dam and its surrounding area were incorporated by preparing a 1 km buffer, resulting in a total analysis area of 198.50 km^2 for flood mapping and LULC assessment. The elevation ranges from sea level to 242 m above the sea level.

Figure 1

Location of the Study Area

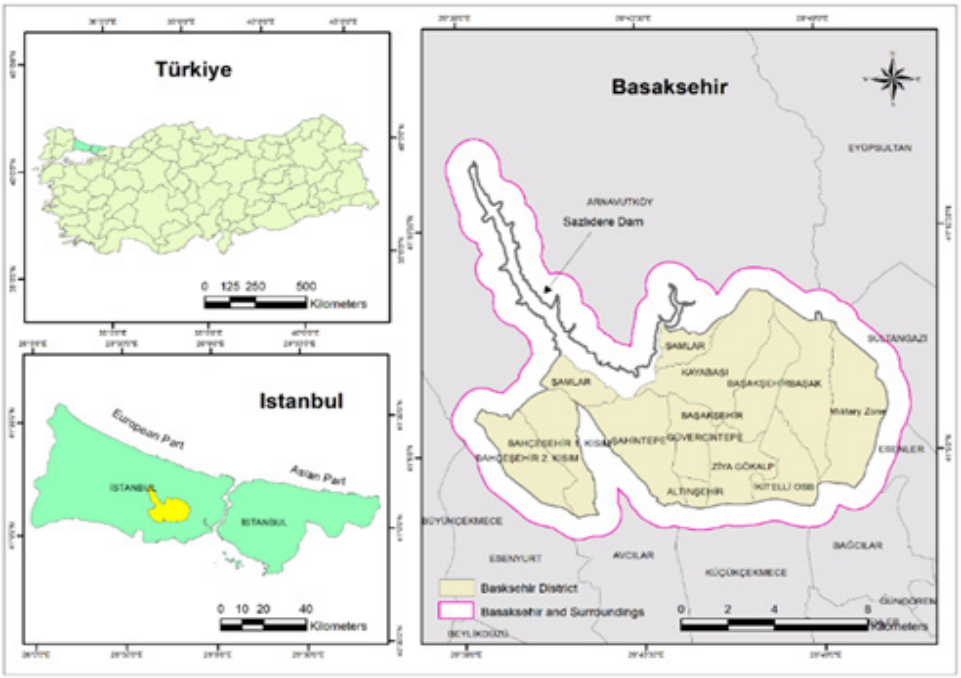

Başakşehir is one of the oldest districts in Istanbul. The district's drinking water is supplied by the Sazlıdere Dam, which has a total water holding capacity of 91.3 hm^3 and provides 50 hm^3 of drinking water to the population (Yilmaz, 2018). The district is situated in proximity to a major motorway (O3), which forms part of the E80 European route, which is the major route to connect with European country Bulgaria in the west. The district is situated within the Marmara region, where it experiences a considerable amount of rainfall and has a maritime and subtropical climate (Yavuz et al., 2022). In the 1950–2022 period, the average annual precipitation was 660.9 mm, with the highest daily values of 136.1 mm recorded in 1981 (Turkish State Meteorological Service, 2024). Additionally, minor snowfall is documented during the period of December to March (Republic of Turkey Governorship of Istanbul, 2024).

2.2. Data

In this study, Sentinel 1A Synthetic Aperture Radar (SAR) satellite and optical Landsat 9 satellite datasets were used to analyse the flood impact on the land use land cover (LULC) for Başakşehir and its surroundings (Table 1). Since Sazlıdere Dam and its surrounding drainage environment are hydrologically relevant to the study area, they were incorporated into the spatial analysis by creating a 1 km buffer in ArcGIS. This buffer was not intended to delineate the full natural watershed, but to include the immediate hydrological context influencing the observed inundation pattern around Başakşehir. The administrative boundary was retained for the calculation of exposure, vulnerability, and relative risk because population, built-up areas, and planning responsibilities are organized and reported at the municipal and subdistrict levels. The digital elevation model (DEM) was prepared to interpret the elevation pattern of the study area and to support the discussion of terrain-controlled flood accumulation. Although elevation-related parameters such as slope, flow accumulation, and distance to drainage or dam structures are important for physically based flood modelling, these variables were used in this study as interpretative spatial indicators rather than as independent parameters in a predictive hydrological model.

Table 1

Satellite Datasets Used in this Study

Satellite Dataset	Acquisition Date	Source	Spatial Resolution
Sentinel–1A	Aug. 10, 2023	ESA	10 m
Sentinel–1A	Sep. 4, 2023	ESA	10 m
Landsat 9	July 2, 2023	USGS	30 m

The precipitation analysis was performed to look into the possible factors responsible for the flooding conditions in the region. Temperature datasets for the period between 2018 and 2023 were analysed and correlated with the precipitation datasets to understand the meteorological variation in the region. A flow chart of the methodology employed is represented in Figure 2.

Figure 2

Flow Chart Representing the Methodology Adopted in the Present Study

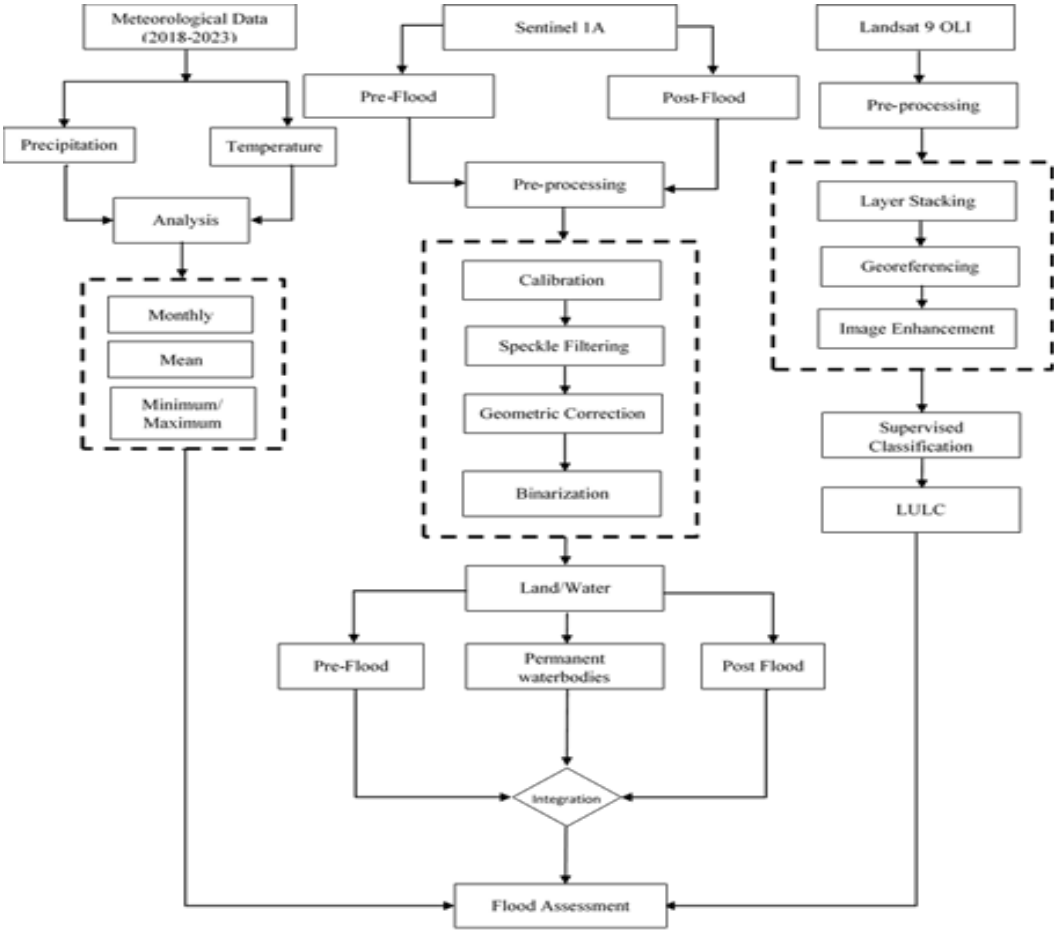

The flood map was prepared using Sentinel-1 SAR satellite images obtained from the European Space Agency (ESA) portal. In this process, the flooded areas were identified through a comparative assessment of pre-flood period (August 10, 2023) and images taken during flood (September 4, 2023) using SAR images. This approach involved comparing pre- and post-flood SAR images to identify permanent water bodies (pre) and floodwater (post), using SNAP software. Pre-processing of the Sentinel-1A datasets was subjected to a series of pre-processing steps, including calibration, speckle filtering, and geometric correction. Binarization was then performed to extract the water pixels, with the threshold set to − 23.7dB, as this method has been considered the most suitable for precise flood mapping using SAR datasets (Cao et al., 2019; Matgen et al., 2011; Tripathi et al., 2019). Moreover, the difference between the flood pixels derived from the pre-flood and post-flood images facilitated the estimation of the flooded areas. This method has been established to be one of the most effective for hydrological analysis by several researchers (Iervolino et al., 2016; Wu & Chau, 2011). Landsat 9 satellite image of July 2, 2023 was considered for the pre-flood land use land cover analysis (LULC) for Başakşehir and its surroundings.

The Landsat 9 satellite data were acquired from the EarthExplorer website, followed by pre-processing of the dataset and clipping of the study area boundary using Erdas Imagine software. The supervised classification method was used by applying the maximum likelihood algorithm to prepare five classes such as terrestrial vegetation, fallow, waterbodies, agriculture, and built-up. The terrestrial vegetation class encompasses all forest areas, including deciduous forest and scrub forest, and the fallow land classes are uncultivated lands left for a specified period of time in order to enhance the productivity and eradicate weeds. Waterbodies comprise surface waterbodies like lakes, rivers, and ponds, whereas the agriculture class encompasses cultivated areas. The built-up class comprises pervious and concrete areas, including buildings, bus stations, railways, and road networks. The maximum number of training sets leads to better classification, so 94 training sets were collected for each class (Palaniswami et al., 2006).

The accuracy assessment was performed for LULC and the flood map using Kappa coefficient techniques that represented an overall accuracy range from 90% to 92% with kappa coefficients of 0.601–0.825 (Peng et al., 2008). The obtained accuracy is suitable for further calculations for raster layers (Ahmad et al., 2020; Anderson, 1976). The five classes of area statistics were subsequently analysed in order to deduce the flood inundation on various LULC classes within the GIS environment. The flood hazard and flood risk analyses were performed with the help of population datasets and the municipal boundary for Başakşehir (Rana & Routray, 2018). The DEM was prepared using ArcGIS with the help of satellite images obtained from the Turkish portal (Harita Genel Müdürlüğü, 2021) to understand the depression areas more feasible to flooding. Flooding map overlaying helps to understand the sinking areas that are more vulnerable to flooding.

2.3. Event-based flood hazard, vulnerability, and relative risk mapping

In this study, event-based flood hazard, flood vulnerability, and relative flood risk indicators were calculated in the GIS environment for the Başakşehir District. These indicators were designed to represent the spatial distribution of observed flood impacts and exposed population, rather than to simulate flood propagation or predict future inundation under different hydrological scenarios. GIS techniques were used to spatially represent several local indicators, including subdistrict inundation, built-up inundation, population distribution and density, flood hazard, vulnerability, and relative risk. Further, the spatial distribution performed for Başakşehir District was categorised into four categories: low, medium, high, and very high using the geospatial method by applying the natural breaking values classification method. Population density is calculated as the total population to the total area of a particular subdistrict (Equation 1).

$$\text{Population Density} = \frac{\text{Population of District}}{\text{Area of District}} \qquad (1)$$

The flood hazard indicator was defined as the ratio of the flood-affected area to the total area of the respective subdistrict (Equation 2). This indicator represents the relative spatial intensity of the observed flood event at the subdistrict scale. It does not represent a physically based hydraulic hazard index, since flood depth, flow velocity, slope, flow accumulation, and distance to river or dam

structures were not mathematically integrated into the hazard equation.

$$\text{Flood Hazard} = \frac{\text{Flood inundation}}{\text{Area of District}} \quad (2)$$

Flood vulnerability was calculated as the ratio of the flood-affected population to the total population of the respective subdistrict (Equation 3).

$$\text{Flood Vulnerability} = \frac{\text{Population affected}}{\text{Total population}} \quad (3)$$

The calculation of the population affected was deduced by the percentage of built-up inundated during the flooding, whereas the built-up area was calculated from satellite images using the supervised classification method. The flood risk was calculated with the help of calculated values of the flood hazard and vulnerability, respectively, represented in Equation 4 (Ahmad et al., 2019; Armenakis et al., 2017; FLOODsite, 2009; Rana & Routray, 2018).

$$\text{Risk} = \text{Flood Hazard} \times \text{Flood Vulnerability} \quad (4)$$

The utilization of a ratio-based hazard indicator is deemed suitable for the identification of relative variations in observed inundation among subdistricts; nevertheless, it is important to acknowledge its inherent limitations. The development of a more comprehensive predictive flood hazard index would necessitate the mathematical integration of additional hydrological and topographic parameters, including elevation, slope, flow accumulation, drainage density, and distance to river or dam systems. The integration of these models would be further enhanced by the implementation of physically based models such as HEC-RAS, HEC-HMS, or SWMM. Given the focus of the present study on satellite-observed inundation and its spatial impacts, these parameters were considered in the interpretation of flood-prone areas but were not incorporated as independent variables in a hydrodynamic simulation.

3. Results and Discussion

3.1. Meteorological data analysis

The meteorological data analysis was performed using monthly precipitation and temperature to ascertain the extent of its variation over a period of six years (2018–2023) for the Başakşehir region and its surrounding areas obtained from the Turkish State Meteorological Service (Meteoroloji Genel Müdürlüğü, 2021). The meteorological analysis for the specific period is a prominent method for understanding the sudden fluctuations in the datasets (Ahmad et al., 2023; Chandniha et al., 2017). A monthly precipitation analysis was conducted to calculate the mean, while the minimum, maximum, and monthly mean values were calculated for the temperature datasets using Microsoft Excel sheets.

An anomaly for the precipitation data was performed to understand the sudden high precipitation in the region. The monthly precipitation for the 12 stations located in the region (Figure 3) was analysed. It was observed that there were eight events of high precipitation (150–200 mm) and four events of very high precipitation (>200 mm) in 2018. In contrast, there was only one event of high precipitation (158 mm) in 2019, followed by three events of high precipitation in 2020. In 2021, six events of high precipitation and one event of very high precipitation were observed, followed by two events of high precipitation and one event of very high precipitation in 2022. In 2023, two events of high precipitation were recorded, with nine events of very high precipitation observed.

Such exceptionally high precipitation was observed in the month of November but only in one instance, which was monitored in September with an amount of 354 mm at the Arnavutköy Rainfall Station. This precipitation event became the primary cause of the flooding conditions in Başakşehir. A review of data from the previous five years revealed that this type of precipitation was an anomaly; as such, high precipitation was not previously observed, with the recorded amount being approximately four times the average precipitation. This variation may also be attributed to other meteorological factors responsible for flooding in the region.

Figure 3

Location of Meteorological Stations

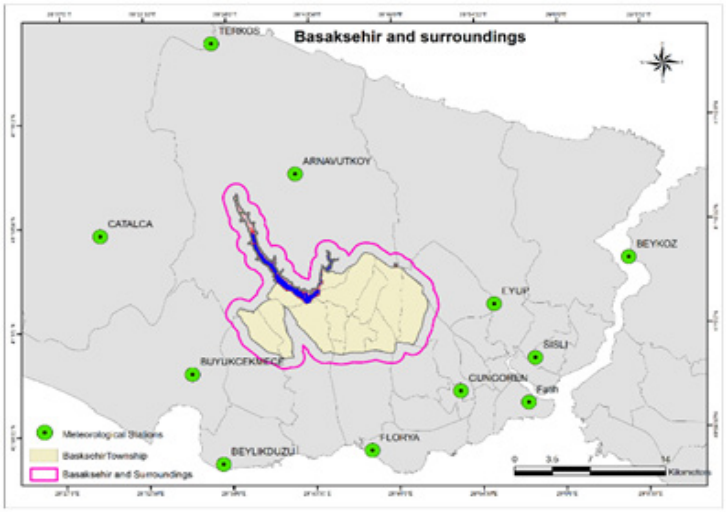

Temperature data for the period of six years (2018–2023) were analysed on a monthly basis to calculate the minimum, maximum, and mean temperatures for the 12 stations. It was observed that August was the hottest month in the last 6 years, with all the stations following with July and June (Figures 4 & 5). The mean temperature observed at Beylikdüzü Station was the highest (26.4 °C) for the month of August, with a mean minimum and maximum of 25.4 °C and 27.7 °C, respectively. The mean precipitation for the month was 5.8 mm, which was the lowest in August. Additionally, it was observed that the mean temperature for all stations monitored was above 20 °C during the months of June to September, which represents the summer season. However, it is notable that the Arnavutköy and Fatih Stations exhibited exceptional mean high precipitation, with values of 97 mm and 128.2 mm, respectively.

Figure 4

The Monthly Precipitation in Başakşehir and the Surroundings Between 2018 and 2023

Figure 5

Monthly Mean, Max., Min. Temperatures, and Precipitation Between 2018 and 2023

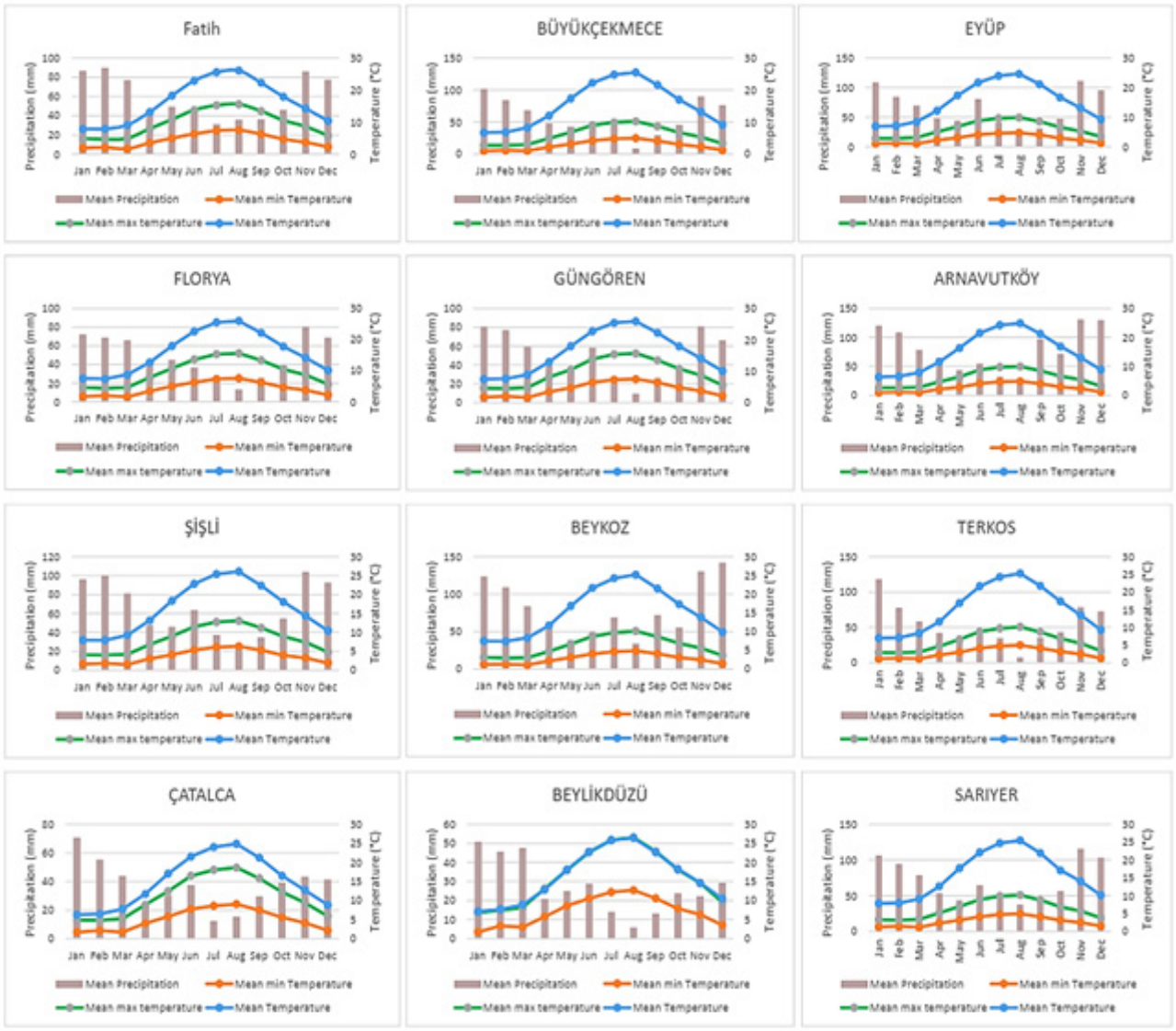

The six-year anomaly shows an increasing trend in the precipitation pattern in all gauge stations. Fatih Gauge Station observed high anomalies in the years 2018, 2019, and 2021; among them, January, June, July, August, September, November, and December received a higher rate of precipitation, while the other period received a lower rate of precipitation or below average precipitation. On the other hand, Büyükçekmece Station recorded high anomalies in the years 2020, 2021, 2022, and 2023. The highest rate of precipitation was recorded in the station in November 2023, while the lowest precipitation was recorded in the same year in January. Notably, July and September also recorded higher anomalies at the station. Eyup Station received high anomalies in the months of January, June, July, August, November, and December, while 2023 contributed to a higher rate of precipitation in the month of November, followed by 2020 in January and 2018 in June, while September recorded negative anomalies at this station, except for the year 2018. Fatih, Büyükçekmece, Florya, and Güngören Stations also recorded a higher rate of anomaly in November 2023, whereas Arnavutköy Station recorded a high anomaly in 2023 in September. These findings depict that the year 2023 was more likely to create flooding conditions, followed by 2018 and 2020. In addition, the period between November and January contributed a higher rate of rainfall, followed by June to July (Figure 6).

Figure 6

Monthly Precipitation Anomaly Patterns Between 2018 and 2023

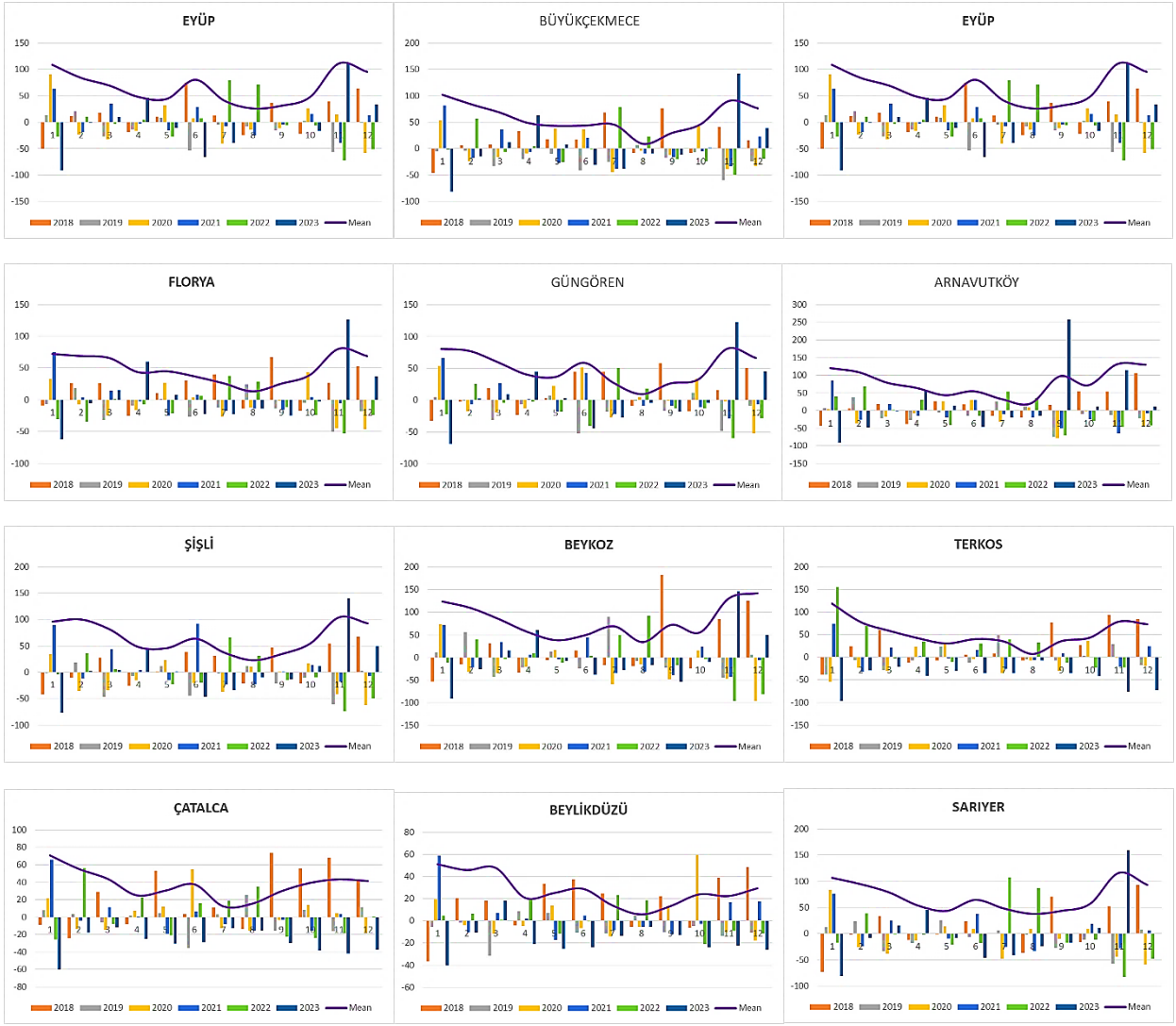

3.2. Flood inundation calculation

Sentinel-1 SAR satellite images were used to quantify the extent of flooding areas in Başakşehir and its surroundings. In this process, permanent waterbodies were calculated using pre-flood images, and 24.90 km^2 was found (Figure 7a), while, during floods, there is estimated to be a 20.28 km^2 increase in the waterbody, which indicates inundated land (Figure 7b). It was observed that the floodwater when mixed with permanent waterbodies became a bulk of waterbodies and found its way towards the depression areas. Consequently, the total water-covered area during the flood period, including permanent waterbodies and newly inundated surfaces, was calculated to be 45.18 km^2. The difference between the pre-flood and flood-period water extent was used to interpret the spatial footprint of the observed flood event (Figure 7c). The permanent waterbodies were predominantly situated in the vicinity of Sazlıdere Dam and sparsely distributed in the northern and western regions. The floodwater was observed to be uniformly distributed throughout the region majorly concentrated in the central and northern parts of Başakşehir.

Figure 7

Flood Mapping for Başakşehir and its Surroundings

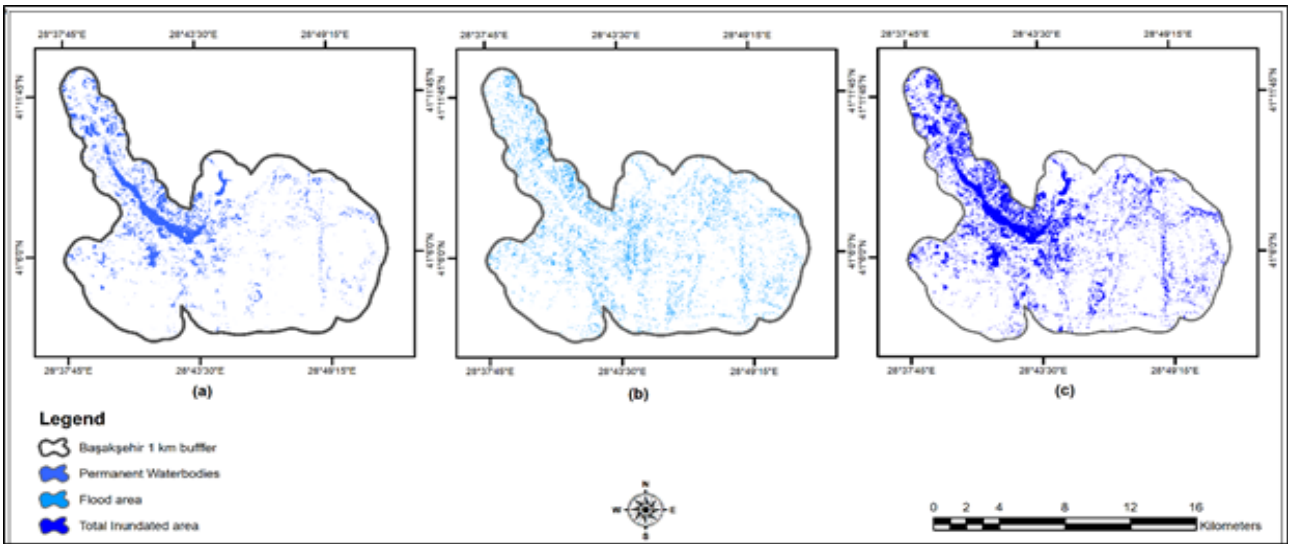

With the help of the dam gauge data, it was observed that the water level was 8–13 m during the month of September, which was below the previous month (Figure 8).

Figure 8

Sazlıdere Dam Data for 2023

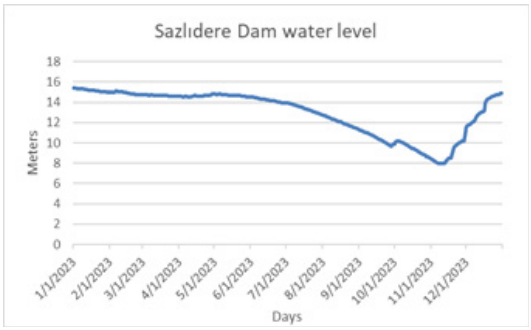

The maximum depth of Sazlıdere Dam is 22.4 m (Yilmaz, 2018), so, during the month of September, there was no higher reading observed in the dam gauge data, which had no role in the flooding conditions in Başakşehir District. Probably, urbanisation could play a major role in the flooding of the region. Therefore, LULC classification has been performed for the study area.

3.3. Land use land cover classification and flood impacts

The Land use land cover play a significant role for comprehensive flood analysis. In this study, LULC classification was prepared for a total area of 198.50 km2, in which five classes were prepared. In the total area, 77.27 km2 area was observed as built-up (38.9% of total area), followed by agriculture area covering 55.14 km2 (27.8%), terrestrial vegetation (37.79 km2; 19%), fallow (23.37 km2; 11.8%), and waterbodies covering 4.93 km2 (2.5% of total area) (Table 2).

Table 2

LULC Classification and Flood Inundation Statistics

Classes	July 2, 2023		September 4, 2023	
	Area (km^2)	LULC (%)	Flood Inundation	Inundation (%)
Vegetation	37.79	19.0	3.41	7.5
Fallow	23.37	11.8	15.80	35.0
Agriculture	55.14	27.8	12.92	28.6
Built-up	77.27	38.9	8.13	18.0
Waterbody	4.93	2.5	4.93	10.9
	198.5	**100.0**	**45.18**	**100.0**

It is observed that built-up land is the most dominant land cover in the study area, followed by terrestrial vegetation, which was significantly observed in the northern, eastern, and some other parts of the study area. Fallow land and agricultural areas were found across the town, with the majority of these areas concentrated in the western and northern parts near Sazlıdere Dam. Overlay analysis of the flood inundation map with the LULC classified map (Figure 9) revealed the impact of floods on the LULC classes. It was observed that fallow land was severely affected during the flood, covering 15.80 km2 (35% of the total inundation), followed by agriculture land, which was inundated by 12.92 km2 (28.6% of the total inundation). This indicated that more than 60% of the inundation was observed in the fallow and agriculture areas (28.72 km2). The inundation of built-up areas was calculated to be 8.13 km2 (18%), which is a considerable amount of inundation for the metropolitan area of the city. The specific characteristics of the topography of the town also became a significant contributing factor to the inundation, as the floodwater flows towards the sinking areas. The considerable volume of floodwater resulted in the area becoming impassable, with the floodwater remaining for days. The DEM indicates that the central and southern regions of Başakşehir are situated in a low-lying area, whereas the northeastern region is at a higher elevation (Figure 10).

Figure 9

Landsat 9 Satellite Image 2023 (a), LULC Classified Map (b)

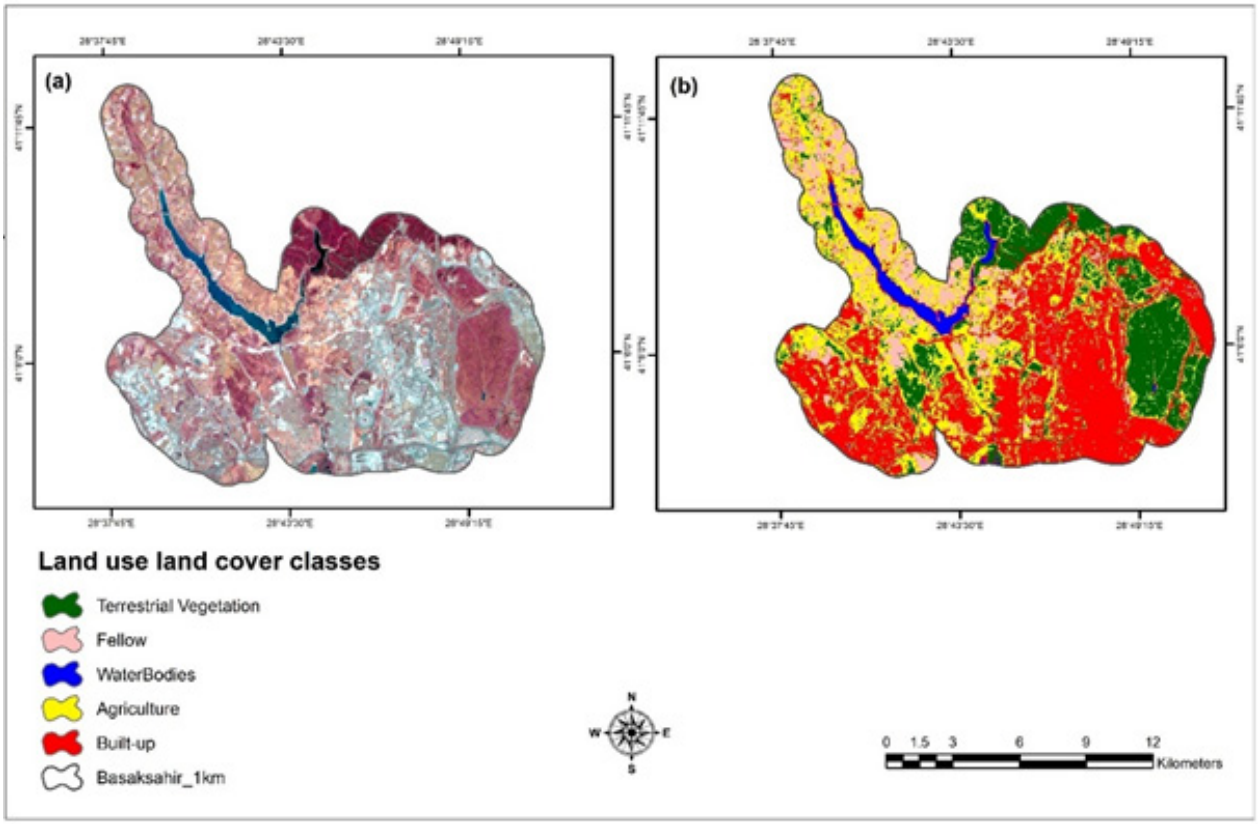

DEM data analysis, along with a field visit of the study area, resulted in a better understanding of the region's geomorphology. This revealed that elevation ranges between 0 and 242 m a.s.l., which provided an additional force and facilitated the drainage of floodwater towards the low-lying region. The variation in elevation results in the movement of floodwater at high speeds, which can lead to urban flooding in the region.

Figure 10

Study Area With 1 Km Buffer Area (a); Built-Up Area (b); DEM (c); Field Points (d)

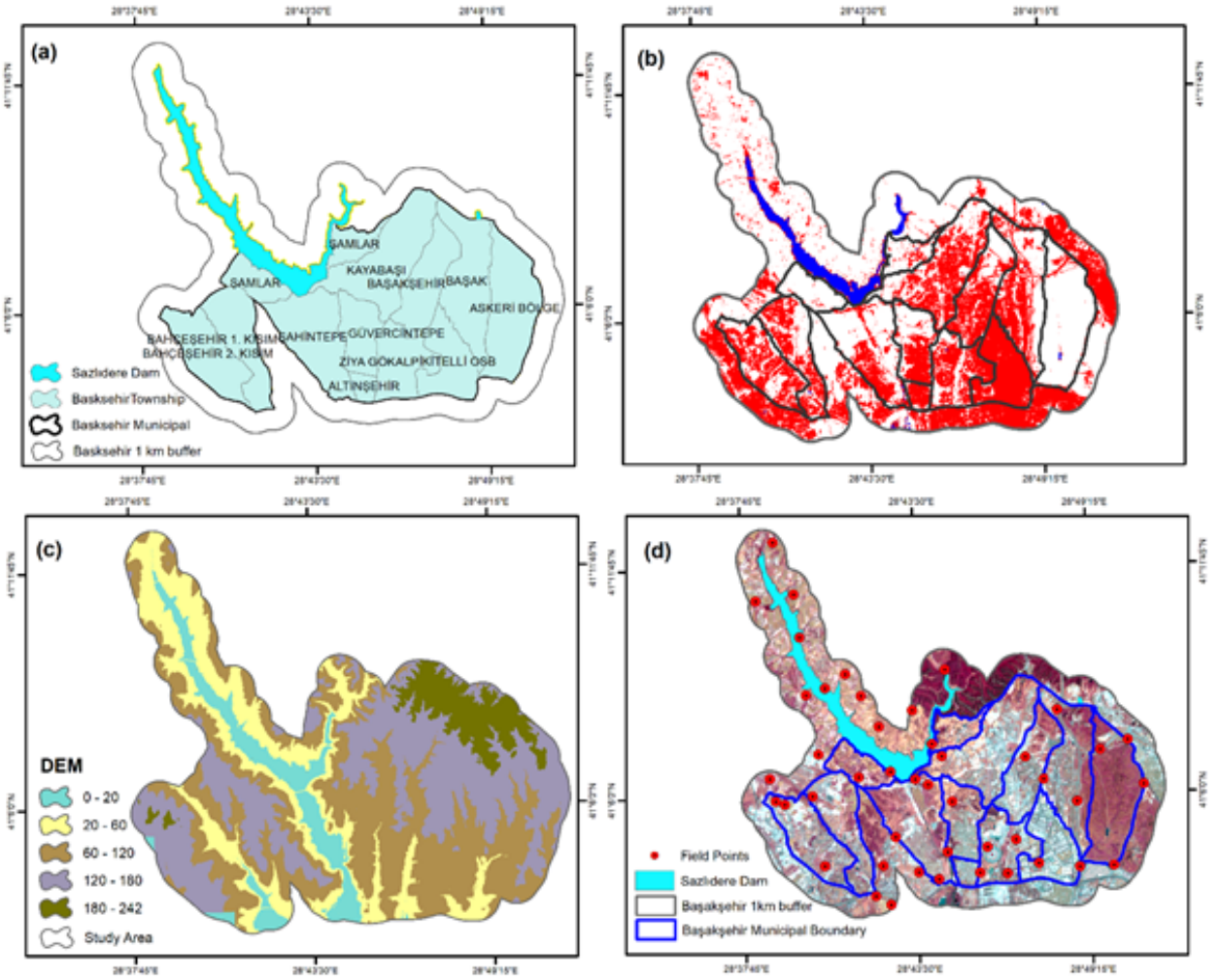

3.4. Event-based flood hazard, vulnerability, and relative risk assessment

In this section, event-based flood hazard, vulnerability, and relative risk indicators were calculated in the GIS environment for the Başakşehir District of Istanbul. These indicators were based on the spatial extent of the observed flood event, built-up exposure, and population distribution, and should therefore be interpreted as relative spatial indicators rather than predictive hydrodynamic outputs. GIS techniques have been employed to represent local indicators for different categories on a spatial basis, with several being excluded, namely the inundation of subdistricts and built-ups, population distribution and density, flood hazard, vulnerability, and risk. The flood hazard indicator for each subdistrict was calculated by estimating the proportion of the subdistrict affected by the observed flood extent. This ratio-based approach enables comparison among subdistricts but does not simulate flood depth, velocity, return period, drainage capacity, or future flood scenarios. The flood hazard analysis revealed that four subdistricts were under the low hazard category (0–11), in which two subdistricts (Altınşehir & İkitelli Osb) were in the southern part of the town and one in the eastern (military zone) and western (Bahçeşehir 2. Kısım) parts of the district. It was observed that six subdistricts (Bahçeşehir 1. Kısım, Kayabaşı, Başakşehir, Başak, Güvercintepe & Ziya Gökalp) were under a moderate flood hazard (11–22) located in the central parts and surroundings. The high hazard (22–32) subdistricts were also located in the central part of the town (Şahintepe), whereas the very high hazard (>32) (Şamlar) was located in the northern part near the Sazlıdere Dam.

Table 3

Statistical Representation of the Pop. Density, Flood Hazard, Vulnerability, and Risk

Subdistrict Name	Area (km^2)	Pop.	Urban Density	Area Under Flood (km^2)	Total Built-Up Area (km^2)	Built-Up Area Under Flood (km^2)	Population Affected by Flood	Flood Hazard	Flood Vulnerability	Flood Risk
Altınşehir	1.36	24,901	23,270	0.03	1.07	0.02	382	2.33	1.53	0.04
Bahçeşehir 1. Kısım	8.32	36,693	8571	1.46	4.28	0.27	2316	17.59	6.31	1.11
Bahçeşehir 2. Kısım	8.68	60,171	12,160	0.60	4.95	0.10	1182	6.89	1.96	0.14
Başak	12.08	70,758	12,233	2.02	5.78	1.10	13,474	16.69	19.04	3.18
Başakşehir	8.13	71,096	14,300	1.14	4.97	0.53	7599	14.08	10.69	1.51
Güvercintepe	5.93	74,234	27,522	0.91	2.70	0.12	3256	15.40	4.39	0.68
İkitelli Osb	7.28	81	11	0.17	7.05	0.15	2	2.40	2.15	0.05
Kayabaşı	13.85	108,455	14,449	2.63	7.51	0.68	9775	18.97	9.01	1.71
Şahintepe	11.56	32,254	8644	2.90	3.73	0.45	3899	25.06	12.09	3.03
Şamlar	7.08	1262	1478	2.88	0.85	0.19	286	40.75	22.68	9.24
Ziya Gökalp	7.35	29,997	6368	1.20	4.71	0.83	5266	16.30	17.55	2.86
Military zone	12.87	NA	NA	1.32	0.92	0.32	NA	10.25	34.93	3.58

The flood vulnerability of each subdistrict was calculated by dividing the population affected by floods by the total population. This figure was then multiplied by the proportion of the built-up area inundated during floods, multiplied by the proportion of the population affected. The analysis revealed the flood vulnerability in five subdistricts (Altınşehir, Bahçeşehir 2. Kısım, Güvercintepe & İkitelli Osb) was low (<6), distributed in the western and southern parts of the district. The three subdistricts (Bahçeşehir 1. Kısım, Kayabaşı & Başakşehir) represent moderate vulnerability (6–12), and three subdistricts (Şahintepe, Ziya Gökalp & Başak) were under the high flood vulnerability category (12–22). Furthermore, it was calculated that Şamlar and the military zone subdistricts were under the very high flood vulnerability category (>22) located in the eastern part of the town.

It has been determined that the spatial multiple of hazard and vulnerability is a pivotal factor in the assessment of flood risk. The study revealed that the Şamlar subdistrict located in the proximity of Sazlıdere Dam and the military zone located in the eastern part of the town were under a very high flood risk (>3.5) (Figure 11). Four subdistricts (Şahintepe, Ziya Gökalp, Başak & Kayabaşı) located in the eastern and southern parts of the town were under a high flood risk category (1.7–3.5). A moderate flood risk (0.6–1.7) was calculated for the three subdistricts (Bahçeşehir 1. Kısım, Güvercintepe & Başakşehir) located in the northern and western parts of the town, whereas low flood risk (<0.6) was computed for the four subdistricts (Altınşehir, Bahçeşehir 2. Kısım & İkitelli Osb) distributed in the southern part.

The results of the study indicate the spatial concentration of observed flood impact and exposed population within the district. However, it is imperative to refrain from interpreting the classification as a deterministic prediction of future flooding events. The absence of a physically based hydrological or hydraulic model hinders the study's capacity to estimate flood depth, flow velocity, temporal flood propagation, and drainage system performance. Therefore, the risk classes presented here should be understood as event-based relative risk zones derived from SAR-observed inundation, LULC, built-up exposure, population distribution, and DEM-supported terrain interpretation. Since the risk indicators were summarized within municipal and subdistrict boundaries, the results are most useful for identifying administrative units requiring priority attention in urban drainage improvement, land-use regulation, and emergency planning. They should not be interpreted as a replacement for watershed-scale hydrological modelling of flood generation and upstream runoff contribution.

Figure 11

Representation of the Flood Hazard, Vulnerability, and Flood Risk for the Başakşehir

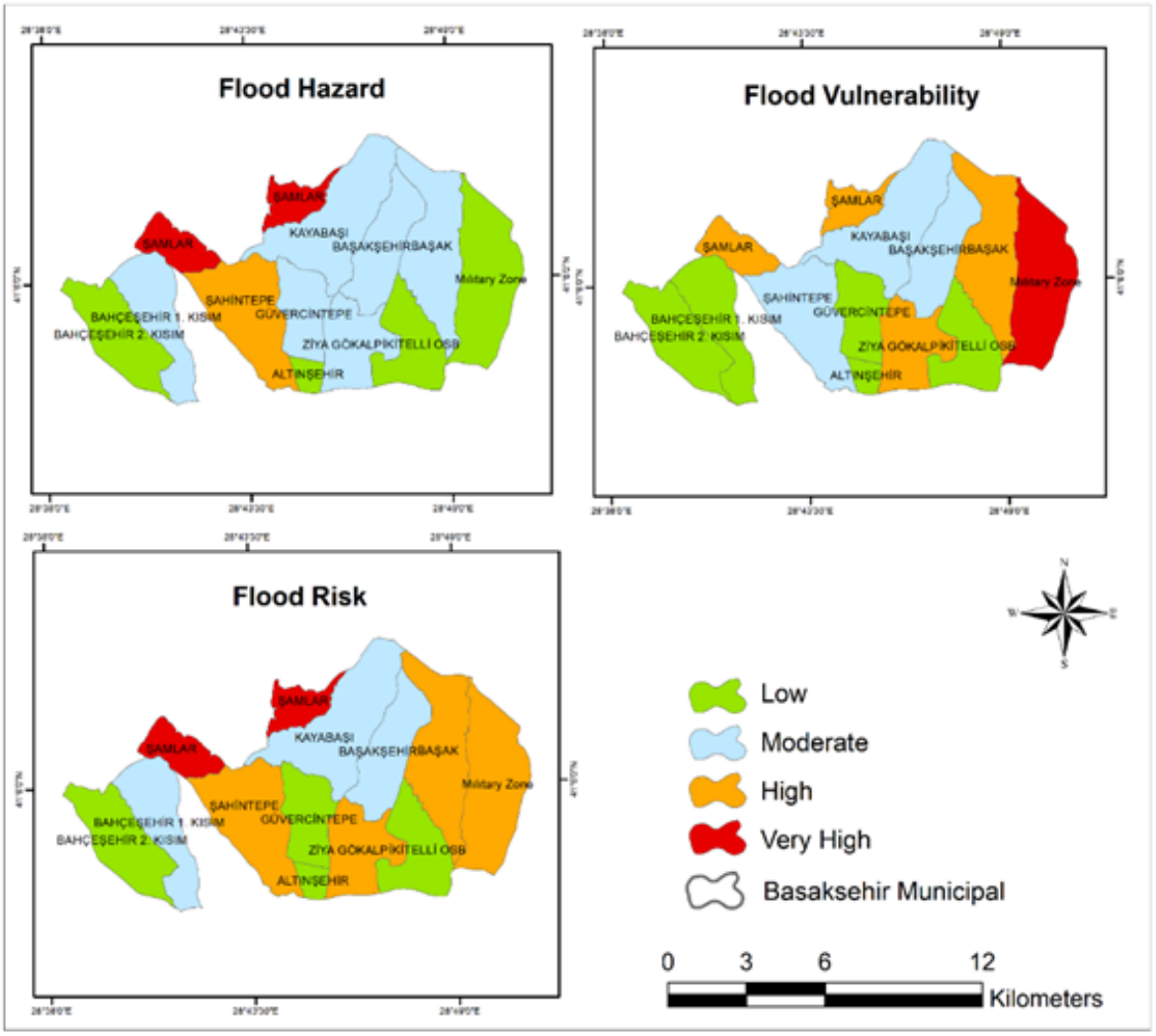

The results of the study indicate the spatial concentration of observed flood impact and exposed population within the district. However, it is imperative to refrain from interpreting the classification as a deterministic prediction of future flooding events. The absence of a physically based hydrological or hydraulic model hinders the study's capacity to estimate flood depth, flow velocity, temporal flood propagation, and drainage system performance. Therefore, the risk classes presented here should be understood as event-based relative risk zones derived from SAR-observed inundation, LULC, built-up exposure, population distribution, and DEM-supported terrain interpretation. Since the risk indicators were summarized within municipal and subdistrict boundaries, the results are most useful for identifying administrative units requiring priority attention in urban drainage improvement, land-use regulation, and emergency planning. They should not be interpreted as a replacement for watershed-scale hydrological modelling of flood generation and upstream runoff contribution.

4. Conclusion

The present study aimed to develop an event-based geospatial assessment of flood inundation, exposure, and relative flood risk, together with an interpretation of meteorological conditions in Başakşehir District of Istanbul and its surroundings. The main contribution of the study lies in integrating SAR-derived permanent and flood-period water extents with LULC, built-up exposure, population data, DEM-supported terrain interpretation, and meteorological records to identify event-based flood exposure and relative risk patterns. The flood analysis revealed that the total permanent waterbodies during pre-flood period (August 10, 2023) was 24.90 km2, which increased to 45.18 km2 during the flooding period of September 4, 2023 using SAR datasets. The floodwater was majorly concentrated in the depression areas located in the central part of Başakşehir and in the vicinity of

Sazlıdere Dam. Looking into the meteorological monthly dataset for 12 stations from 2018 to 2023, it was observed that there were eight events of high precipitation (150–200 mm) and four events of very high precipitation (>200 mm) in 2018 in the region. In contrast, August was the hottest month after June and July, and Beylikdüzü Station had the highest mean temperature of 26.4 °C in August. The exceptionally high precipitation of 354 mm in September at the Arnavutköy rainfall station made it an anomalous month compared to the precipitation observed in the last 5 years.

This paper examines LULC using Landsat 9 satellite images, which shows the dominance of built-up areas covering 38.9% (77.27 km2) concentrated in the central and southern parts of the study area. Agricultural land was mainly observed in the central and eastern parts covering 55.14 km2 (27.8%). The impact of flooding on LULC showed that severe impact was observed in the fallow class with an inundation of 35% (15.8 km2), followed by an agricultural inundation of 28.6% (12.92 km2). As these areas were mostly located in the eastern and northern parts near Sazlıdere Dam, these two classes (fallow & agriculture) accounted for more than 60% of the inundation. The largest inundation of built-up areas was observed in the central part of the region, which was calculated to be 8.13 km2 (18% of the total area). Due to the impermeable concrete surface, which reduces the retention capacity, together with the specific topography, this leads to the high-speed movement of floodwater, which creates urban flooding situations in the city within a very short time. The event-based flood hazard and relative risk assessment performed for Başakşehir within the district boundary showed that one subdistrict (Şamlar) located in the northern part near Sazlıdere Dam was in the very high hazard category. One subdistrict (Şahintepe) located in the central part of Başakşehir was in the high hazard category. Six subdistricts (Bahçeşehir 1. Kısım, Kayabaşı, Başakşehir, Başak, Güvercintepe & Ziya Gökalp) were in the moderate flood hazard category (11–22) located in the central parts and surrounding areas.

The built-up areas in the subdistricts of Başakşehir District were assessed for flood vulnerability. The determination of flood risk showed that one subdistrict (Şamlar) was under a very high flood risk (>3.5), while four subdistricts (Şahintepe, Ziya Gökalp, Başak, and the military zone) located in the eastern and southern parts of the city were under the high flood risk category (1.7–3.5). In contrast, the low flood risk (<0.6) was calculated for the four subdistricts (Bahçeşehir 2. Kısım, Güvercintepe, Altınşehir & İkitelli Osb) located in the southern part of Başakşehir District. This analysis showed that the subdistricts located in the northern part near Sazlıdere Dam are under very high flood risk areas, while the subdistricts located in the depression areas in the central and southern parts are under high flood risk. This understanding could be helpful in the management of the drainage system and the reconstruction of areas built away from the risk zones. In addition to this, the areas located below the height of 60 m should be managed for a proper drainage system for the future flood conditions in the city.

This holistic approach for flood analysis would be beneficial for town planners and researchers to protect the population from the risk zone. The rapid urbanisation has emerged as an important cause of urban flooding in the cities. The study provides a practical event-based geospatial framework for identifying observed flood exposure and relative risk patterns that can support urban planning and disaster management. However, its simplified structure and focus on rapid post-event assessment should be considered among its main limitations. This research can inform strategic town planning, ensuring that infrastructure development considers flood-prone areas, thereby reducing potential damage and reframing the drainage system to enable carrying large amounts of water during high precipitation. Additionally, the methodology can be adapted and applied to other flood-affected regions globally, contributing to more resilient urban environments. Future work could focus on refining hydrometeorological models and incorporating real-time data for even more precise flood forecasting and management.

A notable limitation of the present study is that the flood hazard and risk assessment is based on satellite-observed inundation and GIS-based spatial indicators rather than a physically based hydrodynamic or watershed-scale simulation. Consequently, the findings do not provide estimations of flood depth, flow velocity, return periods, upstream runoff contribution, or the performance of the drainage network. In addition, the use of Başakşehir's administrative boundary limits the ability of the study to fully represent basin-scale hydrogeomorphological processes. Nevertheless, this boundary is appropriate for evaluating observed urban flood exposure and relative risk from the perspective of municipal planning, emergency response, and disaster risk reduction. Future studies should delineate

the relevant watershed boundaries and integrate elevation, slope, flow accumulation, distance to river or dam systems, drainage infrastructure data, and upstream contributing areas into a mathematically weighted flood hazard index. These studies should also validate the results using hydrological or hydraulic models such as HEC-RAS, HEC-HMS, or SWMM.

Article Information Form

Acknowledgments: The authors are thankful to USGS and ESA (for the free availability of satellite datasets), Turkish Statistical Institute, and ISKI for providing auxiliary datasets. The authors are also grateful to Sakarya University for providing a laboratory and infrastructure for the conduction of this research work.

Conflict of Interest Disclosure: No potential conflict of interest was declared by the authors.

Artificial Intelligence Statement: No artificial intelligence tools were used while writing this article.

Plagiarism Statement: This article has been scanned by iThenticate.

References

Abd El Aal, A., Kamel, M., & Al-Homidy, A. (2019). Using remote sensing and GIS techniques in monitoring and mitigation of geohazards in Najran Region, Saudi Arabia. *Geotechnical and Geological Engineering, 37*, 3673–3700. https://doi.org/10.1007/s10706-019-00861-w

Abdel-Fattah, M., Kantoush, S. A., & Sumi, T. (2015). Integrated management of flash flood in wadi system of Egypt: Disaster prevention and water harvesting. *Disaster Prevention Research Institute Annuals. B, 58*, 485–496.

Ahmad, T., Pandey, A. C., & Kumar, A. (2018). Flood hazard vulnerability assessment in Kashmir Valley, India using geospatial approach. *Physics and Chemistry of the Earth, Parts A/B/C, 105*, 59–71. https://doi.org/10.1016/j.pce.2018.02.003

Ahmad, T., Pandey, A. C., & Kumar, A. (2019). Evaluating urban growth and its implication on flood hazard and vulnerability in Srinagar city, Kashmir Valley, using geoinformatics. *Arabian Journal of Geosciences, 12*, Article 308. https://doi.org/10.1007/s12517-019-4458-1

Ahmad, T., Pandey, A. C., & Kumar, A. (2020). Impact of 2014 Kashmir flood on land use/land cover transformation in Dal Lake and its surroundings, Kashmir Valley. *SN Applied Sciences, 2*, Article 681. https://doi.org/10.1007/s42452-020-2434-8

Ahmad, T., Pandey, A. C., Kumar, A., & Tirkey, A. (2023). Understanding the role of surface runoff in potential flood inundation in the Kashmir Valley, western Himalayas. *Physics and Chemistry of the Earth, Parts A/B/C, 131*, Article 103423. https://doi.org/10.1016/j.pce.2023.103423

Anderson, J. R., Hardy, E. E., Roach, J. T., & Witmer, R. E. (1976). *A land use and land cover classification system for use with remote sensor data* (U.S. Geological Survey Professional Paper 964). U.S. Government Printing Office. https://doi.org/10.3133/pp964

Armenakis, C., Du, E., Natesan, S., Persad, R., & Zhang, Y. (2017). Flood risk assessment in urban areas based on spatial analytics and social factors. *Geosciences, 7*(4), Article 123. https://doi.org/10.3390/geosciences7040123

Aslan, Ö. (2022). *Dirençli toplumlardan sorumlu idarelere: İklim temelli aşırı hava olaylarına hak temelli bir yaklaşım*. İstanbul Politikalar Merkezi.

Balaban, M. Ş. (2016). An assessment of flood risk factors in riverine cities of Turkey: Lessons for resilience and urban planning. *METU Journal of the Faculty of Architecture, 33*(2), 45–71. https://doi.org/10.4305/METU.JFA.2016.2.3

Bates, B. C., Kundzewicz, Z. W., Wu, S., & Palutikof, J. P. (Eds.). (2008). *Climate change and water: Technical paper of the Intergovernmental Panel on Climate Change*. Intergovernmental Panel on Climate Change (IPCC) Secretariat.

Bigi, V., Comino, E., Fontana, M., Pezzoli, A., & Rosso, M. (2021). Flood vulnerability analysis in urban context: A socioeconomic sub-indicators overview. *Climate, 9*(1), Article 12. https://doi.org/10.3390/cli9010012

Bubeck, P., Botzen, W. J. W., & Aerts, J. C. J. H. (2012). A review of risk perceptions and other factors that influence flood mitigation behavior. *Risk Analysis, 32*(9), 1481–1495. https://doi.org/10.1111/j.1539-6924.2011.01783.x

Cao, H., Zhang, H., Wang, C., & Zhang, B. (2019). Operational flood detection using Sentinel-1 SAR data over large areas. *Water, 11*(4), Article 786. https://doi.org/10.3390/w11040786

Centre for Research on the Epidemiology of Disasters (CRED). (2022). *EM-DAT documentation*. Retrieved June 16, 2026, from https://doc.emdat.be

Chandniha, S. K., Meshram, S. G., Adamowski, J. F., & Meshram, C. (2017). Trend analysis of precipitation in Jharkhand State, India. *Theoretical and Applied Climatology, 130*, 261–274. https://doi.org/10.1007/s00704-016-1875-x

Chapi, K., Singh, V. P., Shirzadi, A., Shahabi, H., Bui, D. T., Pham, B. T., & Khosravi, K. (2017). A novel hybrid artificial intelligence approach for flood susceptibility assessment. *Environmental Modelling & Software, 95*, 229–245. https://doi.org/10.1016/j.envsoft.2017.06.012

Cloke, H. L., & Pappenberger, F. (2009). Ensemble flood forecasting: A review. *Journal of Hydrology, 375*(3–4), 613–626. https://doi.org/10.1016/j.jhydrol.2009.06.005

Coppock, J. T. (1995). GIS and natural hazards: An overview from a GIS perspective. In A. Carrara & F. Guzzetti (Eds.), *Geographical information systems in assessing natural hazards* (pp. 21–34). Kluwer Academic Publishers. https://doi.org/10.1007/978-94-015-8404-3_2

Coroza, O., Evans, D., & Bishop, I. (1997). Enhancing runoff modeling with GIS. *Landscape and Urban Planning, 38*(1–2), 13–23. https://doi.org/10.1016/S0169-2046(97)00015-7

Dobrovolsky, S. G., Istomina, M. N., & Pasechkina, V. Y. (2018). Changes in the natural parameters of extreme hydrological phenomena in Russia and in the world and the damage caused by them: Floods and droughts. *Issues in Geography, 145*, 183–193.

Elsadek, W. M., Ibrahim, M. G., Mahmod, W. E., & Kanae, S. (2019). Developing an overall assessment map for flood hazard on large area watershed using multi-method approach: Case study of Wadi Qena watershed, Egypt. *Natural Hazards, 95*, 739–767. https://doi.org/10.1007/s11069-018-3517-3

Eshrati, L., Mahmoudzadeh, A., & Taghvaei, M. (2015). Multi hazards risk assessment, a new methodology. *International Journal of Health System and Disaster Management, 3*(2), 79–88.

FLOODsite. (2009). *Flood risk assessment and flood risk management: An introduction and guidance based on experiences and findings of FLOODsite*. Deltares | Delft Hydraulics. https://www.floodsite.net

Gaya, S., & Cherrared, M. (2023). Inundation risk of sewerage system according to the concepts of hazard and vulnerability: Case of Algiers City. *Journal of the Geographical Institute "Jovan Cvijić" SASA, 73*(2), 139–154. https://doi.org/10.2298/IJGI2302139G

Grigorieva, E. A., & Livenets, A. S. (2022). Risks to the health of Russian population from floods and droughts in 2010–2020: A scoping review. *Climate, 10*(3), Article 37. https://doi.org/10.3390/cli10030037

Guo, K., Guan, M., & Yu, D. (2021). Urban surface water flood modelling: A comprehensive review of current models and future challenges. *Hydrology and Earth System Sciences, 25*(5), 2843–2860. https://doi.org/10.5194/hess-25-2843-2021

Hall, J. W., Evans, E. P., Penning-Rowsell, E. C., Sayers, P. B., Thorne, C. R., & Saul, A. J. (2003). Quantified scenarios analysis of drivers and impacts of changing flood risk in England and Wales: 2030–2100. *Global Environmental Change Part B: Environmental Hazards, 5*(3–4), 51–65. https://doi.org/10.1016/j.hazards.2004.04.002

Harita Genel Müdürlüğü (HGM). (2021). *Turkish administrative borders data*. Republic of Türkiye Ministry of National Defense. Retrieved June 16, 2026, from https://www.harita.gov.tr

Hitouri, S., Mohajane, M., Lahsaini, M., Ali, S. A., Setargie, T. A., Tripathi, G., D'Antonio, P., Singh, S. K., & Varasano, A. (2024). Flood susceptibility mapping using SAR data and machine learning algorithms in a small watershed in Northwestern Morocco. *Remote Sensing, 16*(5), Article 858. https://doi.org/10.3390/rs16050858

Hu, P., Zhang, Q., Shi, P., Chen, B., & Fang, J. (2018). Flood-induced mortality across the globe: Spatiotemporal pattern and influencing factors. *Science of the Total Environment, 643*, 171–182. https://doi.org/10.1016/j.scitotenv.2018.06.197

Iervolino, P., Guida, R., & Whittaker, P. (2016). A model for the backscattering from a canonical ship in SAR imagery. *IEEE Journal of Selected Topics in Applied Earth Observations and Remote Sensing, 9*(3), 1163–1175.

Intergovernmental Panel on Climate Change (IPCC). (2023). *Climate change 2021: The physical science basis: Working Group I contribution to the Sixth Assessment Report of the Intergovernmental Panel on Climate Change*. Cambridge University Press. https://doi.org/10.1017/9781009157896

Jonkman, S. N. (2005). Global perspectives on loss of human life caused by floods. *Natural Hazards, 34*, 151–175. https://doi.org/10.1007/s11069-004-8891-3

Koç, G., & Thieken, A. H. (2018). The relevance of flood hazards and impacts in Turkey: What can be learned from different disaster loss databases? *Natural Hazards, 91*, 375–408. https://doi.org/10.1007/s11069-017-3134-6

Korjenić, A., Hrelja, E., Sivac, A., & Banda, A. (2021). Application of GIS in the assessment of flood risk in the Region Zenica-Doboj Canton. *Geographia Technica, 16*(2), 80–94. https://doi.org/10.21163/GT_2021.162.07

Ku, C.-A. (2024). Evaluating the effects of land-use strategies on future flood risk reduction in urban areas. *Cities, 150*, Article 104989. https://doi.org/10.1016/j.cities.2024.104989

Kundzewicz, Z. W., Su, B., Wang, Y., Wang, G., Wang, G., Huang, J., & Jiang, T. (2019). Flood risk in a range of spatial perspectives: From global to local scales. *Natural Hazards and Earth System Sciences, 19*(6), 1319–1328. https://doi.org/10.5194/nhess-19-1319-2019

Kundzewicz, Z. W., Kanae, S., Seneviratne, S. I., Handmer, J., Nicholls, N., Peduzzi, P., Mechler, R., Bouwer, L. M., Arnell, N., Mach, K., Muir-Wood, R., Brakenridge, G. R., Kron, W., Benito, G., Honda, Y., Takahashi, K., & Sherstyukov, B. (2014). Flood risk and climate change: Global and regional perspectives. *Hydrological Sciences Journal, 59*(1), 1–28. https://doi.org/10.1080/02626667.2013.857411

Matgen, P., Hostache, R., Schumann, G., Pfister, L., Hoffmann, L., & Savenije, H. H. G. (2011). Towards an automated SAR-based flood monitoring system: Lessons learned from two case studies. *Physics and Chemistry of the Earth, Parts A/B/C, 36*(7–8), 241–252. https://doi.org/10.1016/j.pce.2010.12.009

Merz, B., Blöschl, G., Vorogushyn, S., Dottori, F., Aerts, J. C. J. H., Bates, P., Bertola, M., Kemter, M., Kreibich, H., Lall, U., & Macdonald, E. (2021). Causes, impacts and patterns of disastrous river floods. *Nature Reviews Earth & Environment, 2*(9), 592–609. https://doi.org/10.1038/s43017-021-00195-3

Messner, F., & Meyer, V. (2006). Flood damage, vulnerability and risk perception: Challenges for flood damage research. In J. Schanze, E. Zeman, & J. Marsalek (Eds.), *Flood risk management: Hazards, vulnerability and mitigation measures* (pp. 149–167). Springer. https://doi.org/10.1007/978-1-4020-4598-1_13

Meteoroloji Genel Müdürlüğü (MGM). (2021). *Precipitation data: Climate data*. Retrieved June 16, 2026, from https://www.mgm.gov.tr

Mishra, A., Mukherjee, S., Merz, B., Singh, V. P., Wright, D. B., Villarini, G., Paul, S., Kumar, D. N., Khedun, C. P., Niyogi, D., Schumann, G., & Stedinger, J. R. (2022). An overview of flood concepts, challenges, and future directions. *Journal of Hydrologic Engineering, 27*(6), Article 03122001. https://doi.org/10.1061/(ASCE)HE.1943-5584.0002164

Murray, V., & Ebi, K. L. (2012). IPCC special report on managing the risks of extreme events and disasters to advance climate change adaptation (SREX). *Journal of Epidemiology and Community Health, 66*(9), 759–760. https://doi.org/10.1136/jech-2012-201045

Ologunorisa, T. E., Obioma, O., & Eludoyin, A. O. (2022). Urban flood event and associated damage in the Benue Valley, Nigeria. *Natural Hazards, 111*, 261–282. https://doi.org/10.1007/s11069-021-05052-6

Palaniswami, C., Upadhyay, A. K., & Maheswarappa, H. P. (2006). Spectral mixture analysis for subpixel classification of coconut. *Current Science, 91*(12), 1706–1711.

Parida, B. R., Tripathi, G., Pandey, A. C., & Kumar, A. (2022). Estimating floodwater depth using SAR-derived flood inundation maps and geomorphic model in Kosi River Basin, India. *Geocarto International, 37*(16), 4336–4360. https://doi.org/10.1080/10106049.2021.1899298

Park, K., Choi, S.-H., & Yu, I. (2021). Risk type analysis of building on urban flood damage. *Water, 13*(18), Article 2505. https://doi.org/10.3390/w13182505

Peduzzi, P., Dao, H., Herold, C., & Mouton, F. (2009). Assessing global exposure and vulnerability towards natural hazards: The Disaster Risk Index. *Natural Hazards and Earth System Sciences, 9*(4), 1149–1159. https://doi.org/10.5194/nhess-9-1149-2009

Peng, J., Wu, J., Yin, H., Li, Z., Chang, Q., & Mu, T. (2008). Rural land use change during 1986–2002 in Lijiang, China, based on remote sensing and GIS data. *Sensors, 8*(12), 8201–8223. https://doi.org/10.3390/s8128201

Prama, M., Omran, A., Schröder, D., & Abouelmagd, A. (2020). Vulnerability assessment of flash floods in Wadi Dahab Basin, Egypt. *Environmental Earth Sciences, 79*, Article 114. https://doi.org/10.1007/s12665-020-8860-5

Prokop, P., Wiejaczka, Ł., Sarkar, S., Bryndal, T., Bucała-Hrabia, A., Kroczak, R., Soja, R., & Płaczkowska, E. (2020). Morphological and sedimentological responses of small stream channels to extreme rainfall and land use in the Darjeeling Himalayas. *Catena, 188*, Article 104444. https://doi.org/10.1016/j.catena.2019.104444

Rana, I. A., & Routray, J. K. (2018). Integrated methodology for flood risk assessment and application in urban communities of Pakistan. *Natural Hazards, 91*, 239–266. https://doi.org/10.1007/s11069-017-3124-8

Rashwan, M., Mohamed, A. K., Alshehri, F., Almadani, S., Khattab, M., & Mohamed, L. (2023). Flash flood hazard assessment along the Red Sea coast using remote sensing and GIS techniques. *ISPRS International Journal of Geo-Information, 12*(11), Article 465. https://doi.org/10.3390/ijgi12110465

Republic of Turkey Governorship of Istanbul (RTGI). (2024). *Republic of Turkey Governorship of Istanbul*. Retrieved June 16, 2026.

Shalikovskiy, A., & Kurganovich, K. (2017). Flood hazard and risk assessment in Russia. *Natural Hazards, 88*(Suppl. 1), 133–147. https://doi.org/10.1007/s11069-016-2681-6

Shankman, D., Keim, B. D., & Song, J. (2006). Flood frequency in China's Poyang Lake region: Trends and teleconnections. *International Journal of Climatology, 26*(9), 1255–1266. https://doi.org/10.1002/joc.1307

Shrestha, B. B., & Kawasaki, A. (2020). Quantitative assessment of flood risk with evaluation of the effectiveness of dam operation for flood control: A case of the Bago River Basin of Myanmar. *International Journal of Disaster Risk Reduction, 50*, Article 101707. https://doi.org/10.1016/j.ijdrr.2020.101707

Sinha, R., Bapalu, G. V., Singh, L. K., & Rath, B. (2008). Flood risk analysis in the Kosi River Basin, North Bihar using multi-parametric approach of Analytical Hierarchy Process (AHP). *Journal of the Indian Society of Remote Sensing, 36*, 335–349. https://doi.org/10.1007/s12524-008-0034-y

Tehrany, M. S., Ahmad, B., Mansor, S., & Ahmad, N. (2015). Flood susceptibility assessment using GIS-based support vector machine model with different kernel types. *Catena, 125*, 91–101. https://doi.org/10.1016/j.catena.2014.10.017

Tomar, P., Singh, S. K., Kanga, S., Meraj, G., Kranjčić, N., Đurin, B., & Pattanaik, A. (2021). GIS-based urban flood risk assessment and management: A case study of Delhi National Capital Territory (NCT), India. *Sustainability, 13*(22), Article 12850. https://doi.org/10.3390/su132212850

Tripathi, G., Parida, B. R., & Pandey, A. C. (2019). Spatio-temporal rainfall variability and flood prognosis analysis using satellite data over North Bihar during the August 2017 flood event. *Hydrology, 6*(2), Article 38. https://doi.org/10.3390/hydrology6020038

Turkish State Meteorological Service (TSMS). (2024). *Turkish State Meteorological Service official web sites: Forecast cities—Istanbul*. Retrieved June 16, 2026, from https://www.mgm.gov.tr/eng/forecast-cities.aspx?m=Istanbul

Turkish Statistical Institute (TurkStat). (2023). *Population data from data portal for statistical*. Retrieved June 16, 2026, from https://data.tuik.gov.tr/

United Nations Office for Disaster Risk Reduction (UNDRR). (2015). *The human cost of weather-related disasters 1995–2015*. UNISDR. https://www.unisdr.org/files/46796_cop21weatherdisastersreport2015.pdf

Vázquez-Tarrío, D., Ruiz-Villanueva, V., Garrote, J., Benito, G., Calle, M., Lucía, A., & Díez-Herrero, A. (2024). Effects of sediment transport on flood hazards: Lessons learned and remaining challenges. *Geomorphology, 446*, Article 108976. https://doi.org/10.1016/j.geomorph.2023.108976

Wu, C. L., & Chau, K. W. (2011). Rainfall–runoff modeling using artificial neural network coupled with singular spectrum analysis. *Journal of Hydrology, 399*(3–4), 394–409. https://doi.org/10.1016/j.jhydrol.2011.01.017

Yanmaz, A. M., & Usul, N. (1999). Assessment of flood induced problems of urbanized areas in Turkey. In E. M. Komut (Ed.), *Urban settlements and natural disasters: Proceedings of the UIA Region II Workprogramme Workshop* (pp. 1–8). UIA Region II Workprogramme Workshop.

Yavuz, V., Lupo, A. R., Fox, N. I., & Deniz, A. (2022). The role of short-wave troughs on the formation and development of sea-effect snowbands in the western Black Sea. *Theoretical and Applied Climatology, 149*, 501–510. https://doi.org/10.1007/s00704-022-04071-y

Yilmaz, N. (2018). Assessment of seasonal variation of phytoplankton and related water quality parameters of Sazlıdere Dam Lake (Istanbul, Turkey). *Desalination and Water Treatment, 131*, 107–113. https://doi.org/10.5004/dwt.2018.23011

Zeleňáková, M., Gaňová, L., Purcz, P., Horský, M., Satrapa, L., Blišťan, P., & Diaconu, D. C. (2017). Mitigation of the adverse consequences of floods for human life, infrastructure, and the environment. *Natural Hazards Review, 18*(4), Article 05017002. https://doi.org/10.1061/(ASCE)NH.1527-6996.0000255

Zelenakova, M. (2011). Flood risk assessment and management in Slovak Republic. *Electronic Journal of the Faculty of Civil Engineering Osijek-e-GFOS, 2*(3), 113–119. https://hrcak.srce.hr/74409

Zhao, X., Li, H., Cai, Q., Pan, Y., & Qi, Y. (2023). Managing extreme rainfall and flooding events: A case study of the 20 July 2021 Zhengzhou flood in China. *Climate, 11*(11), Article 228. https://doi.org/10.3390/cli11110228